

UNCLASSIFIED

Defense Technical Information Center
Compilation Part Notice

ADP014282

TITLE: Red Shift in Optical Absorption Tall and Superparamagnetism of gamma-Fe₂O₃ Nanoparticles in a Polymer Matrix

DISTRIBUTION: Approved for public release, distribution unlimited

This paper is part of the following report:

TITLE: Materials Research Society Symposium Proceedings Volume 740
Held in Boston, Massachusetts on December 2-6, 2002. Nanomaterials for
Structural Applications

To order the complete compilation report, use: ADA417952

The component part is provided here to allow users access to individually authored sections of proceedings, annals, symposia, etc. However, the component should be considered within the context of the overall compilation report and not as a stand-alone technical report.

The following component part numbers comprise the compilation report:
ADP014237 thru ADP014305

UNCLASSIFIED

Red Shift in Optical Absorption Tail and Superparamagnetism of γ -Fe₂O₃ Nanoparticles in a Polymer Matrix

John K. Vassiliou¹, Jens W. Otto², V. Mehrotra³ and J. J. Davis¹

¹Department of Physics, Villanova University, Villanova, PA 19085

²Joint Research Center for the European Commission, B-1049 Brussels, Belgium

³RSC Rockwell, Thousand Oaks, CA

ABSTRACT

Well defined spherical particles of γ -Fe₂O₃ have been synthesized in the pores of a polymer matrix in the form of beads by an ion exchange and precipitation reaction. The particle size distribution is a gaussian with an average diameter of 80 Å. The DC magnetic susceptibility and the magnetization of the nanocomposite has been measured between 4 and 300 K using a Faraday balance and a magnetometer, respectively. The magnetic measurements demonstrate that the particles are superparamagnetic with a blocking temperature T_b about 55 K. The optical absorption edge of the mesoscopic system is red shifted with respect to single crystal films of γ -Fe₂O₃ with an absorption tail extended deeply in the gap. Although lattice distortion and existence of excitonic states in the gap can explain the absorption behavior, the red shift can successfully be explained by the quantum confinement of an electron-hole pair in a spherical well.

INTRODUCTION

Nanophases and nanocomposite materials have been the subject of numerous studies¹⁻⁶, because of their interesting physical properties and their potential use to diverse applications such as high density magnetic recording⁷, magnetic refrigeration⁸, ferrofluids⁹ and color imaging¹⁰. This activity has been triggered by the realization that the physical and chemical properties of nanophase materials are usually dramatically different from those of the bulk counterparts and that nanophase materials often exhibit novel or crossover phenomena. As a result of their small size the properties of nanoparticles are intermediate to those of molecules and bulk solids. The magnetic and optical properties of small particles are modified by the particle size effects. Below a certain critical size, magnetic particles become single domain as opposed to multidomain in the bulk¹¹. Furthermore, magnetic nanoparticles exhibit unique phenomena such as superparamagnetism^{12,13}, quantum tunneling of magnetization^{14,16} and occasionally possess unusually high coercivities. Another well known particle size effect is the blue shift of the optical absorption edge in semiconductor nanoparticles¹⁷, due to the molecular character of the wave function of the particles. Novel magnetic and optical properties have been sought by forming nanocomposites of nanoscale magnetic particles in a nonmagnetic matrix in the form of polymer beads^{18,19}. The interplay of particle size and properties is reported here.

EXPERIMENTAL

Nanometer-scale iron oxide magnetic particles were synthesized in the porous network of a cross-linked polymer matrix by ion exchange reaction and subsequent hydrolysis¹⁸. The

polymer matrix is a strongly acidic, cation exchange, resin containing sulfonate functional groups. It consists of sulfonated polystyrene, cross linked with divinylbenzene to form a three dimensional, porous network. We used 50X8-200 resin, marketed under the name Dowex, which is composed of an 8% cross-linked matrix, thus providing a cation exchange capacity of 5.2 meq/g. The polymer was in the form of uniform spherical beads with an approximate diameter of 150 μm . The beads were exposed to an aqueous solution of FeCl_2 , for an hour, and subsequently washed in sodium hydroxide solution for varying times. Finally the beads were washed with deionized water and methanol and dried to 60 degrees.

Energy dispersive X-ray powder diffraction (EDXD) patterns were obtained using synchrotron radiation at the Cornell High Energy Synchrotron Source (CHESS). The data were collected using a solid germanium detector. The particle size and shape of the iron oxide was determined by transmission electron microscopy (TEM) on microtomed samples. The particle size distribution was determined from the TEM images using a graphic particle size analyzer. The DC magnetic susceptibility of the samples was measured between 4.2 and 300 K by the Faraday balance method, at magnetic field strengths ranging from 2 to 10 kG.

Magnetization measurements were performed using a vibrating sample magnetometer with a helium flow cryostat¹⁹, as well as a Squid magnetometer. The zero field cooled measurements were taken by inserting the sample in the cryostat at zero magnetic field and letting the temperature stabilize at 10 K. A magnetic field of 200 G was applied and the magnetization was measured while increasing the temperature. The field cooled measurements were taken by taking the sample out of the cryostat warming it at room temperature and subsequently, inserting it in the cryostat with a magnetic field of 200 G applied and cooled to 10 K. The magnetization measurements were taken by gradually increasing the temperature.

Optical transmission measurements were performed on a single γ - Fe_2O_3 /polymer composite bead using light from a 100 W quartz tungsten-halogen lamp. A single crystal of sapphire was used for mounting the beads. The light from the lamp was monochromated and focused onto a 20 μm spot on the sample. The transmitted light was collected and refocused onto the detector by a sapphire lens. A GaAs photomultiplier tube was used as a detector. A normalized spectrum was taken through the pristine polymer bead¹⁹.

RESULTS AND DISCUSSION

Energy dispersive X-ray scattering identified the oxide phase as γ - Fe_2O_3 (maghemite). The diffraction peaks (Fig.1) were superimposed on a broad background from the amorphous polymer. The pattern was indexed for a cubic phase corresponding to the spinel structure $O_h^7 - Fd\bar{3}m$. It could also be indexed for the tetragonal phase $P4_1 - C_4^2$. The lattice parameters obtained for the tetragonal phase are $a=8.25 \text{ \AA}$ (8.34 \AA) and $c=25.48 \text{ \AA}$ (25.02 \AA). The values in the parenthesis are the lattice parameters reported in the literature. The pristine beads were X-ray amorphous. Electron diffraction patterns demonstrated the crystalline nature of the particles. Transmission electron micrographs in conjunction with a particle size analyzer determined the particle size distribution to be gaussian with a particle mean radius of 42.5 \AA and a standard deviation of 10 \AA . Magnetization measurements as function of magnetic field demonstrate that the composite is superparamagnetic between room temperature and 50 K (Fig.2,3). Below 50 K an hysteresis loop appears. The magnetic susceptibility of the nanocomposite depends upon the particle size and the strength of the magnetic field. It increases with decreasing temperature and

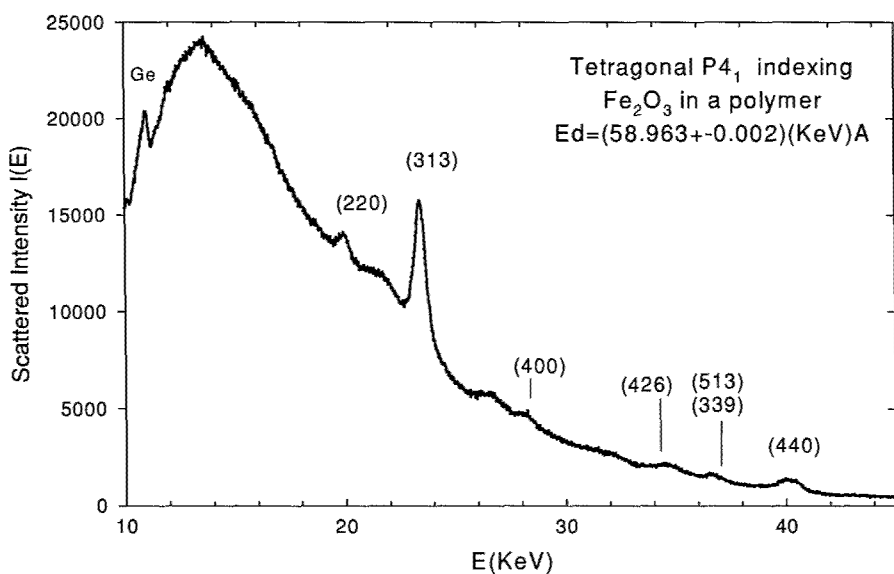


Fig.1. Energy dispersive X-ray pattern of γ - Fe_2O_3 in a polymer matrix. The indexing corresponds to the tetragonal $P4_1$ crystal group

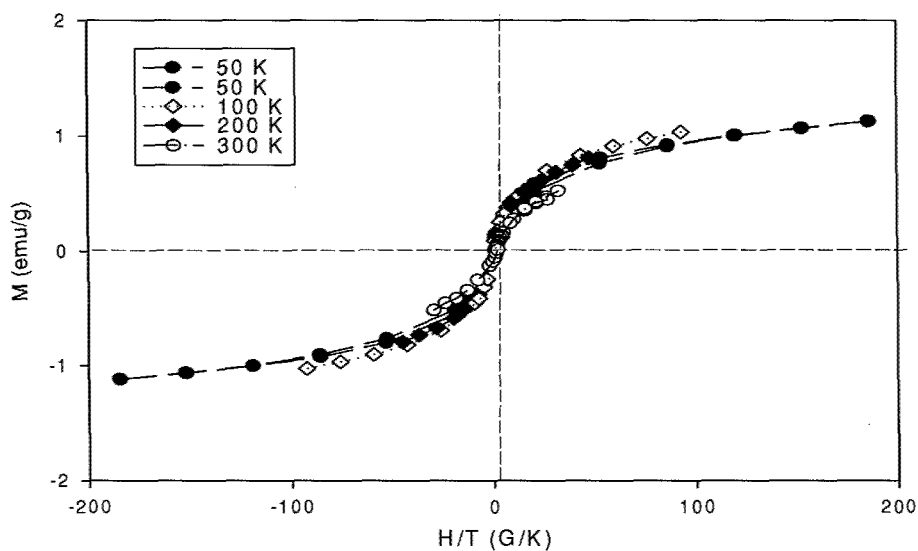


Fig.2. The H/T superposition of all magnetization data for temperatures T greater than the blocking temperature T_b demonstrating superparamagnetic behavior

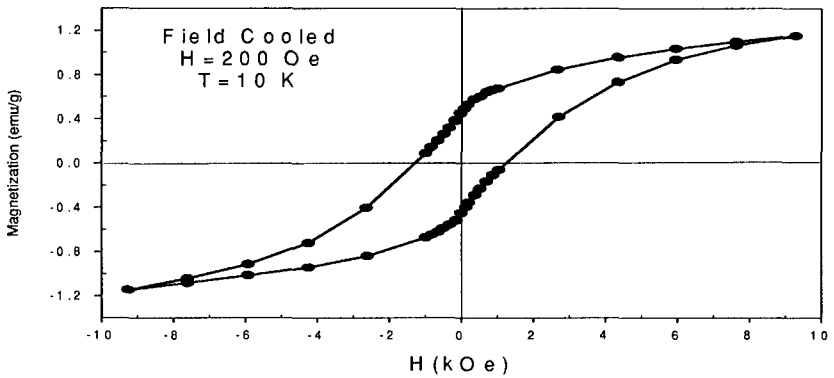


Fig. 3. Magnetization versus applied magnetic field for field cooled loop at 10 K

saturates at low temperatures. The magnitude of the susceptibility is reduced with increasing magnetic field, while the temperature dependance is unaltered¹⁹.

The optical absorption (Fig.4) appears to be red shifted by 0.2 eV in relation to the energy gap of a crystalline film of γ -Fe₂O₃ on MgO²⁰. The optical absorption tail penetrates deeply in the energy gap, suggesting the existence of localized energy states in the gap or indirect transitions. The localized states may be due to disorder, impurities, surface states or excitonic states. For a direct allowed optical transition from the valence band to the conduction band the absorption is given by the equation $a = C(E_{pt} - E_g)^{1/2}$ where E_{pt} is the photon energy and E_g is the direct energy gap. For indirect transitions, when direct transitions are allowed, the absorption of a photon is accompanied by the absorption or emission of a phonon. The absorption is given by the following equation

$a = C_+(E_{pt} - h\nu_{pn} - E_{g1})^2 + C_-(E_{pt} + h\nu_{pn} - E_{g1})^2$, where $h\nu_{pn}$ is the phonon energy and ν_{pn} and h are the phonon frequency and the Planck's constant respectively. If we plot the square of the absorption versus photon energy we find the direct energy gap to be $E_g = 2.02$ eV. By plotting the square root of the absorption tail penetrating the gap below 2.02 eV we can find the indirect energy gap $E_{g1} = 1.64$ eV and the involved phonon energy $E_{pn} = 0.04$ eV. The involved phonon's frequency is $\nu_{pn} = 9.8$ THz.

The red shift of the optical absorption can successfully be explained by the quantum size effects of an electron-hole pair confined in a semiconductor nanoparticle²¹⁻²³. The energy gap E_g of a particle of radius R is determined by the following equation:

$$E_g(R) = E_g^0 + \frac{\hbar^2 \pi^2}{2\mu R^2} - \frac{1.786e^2}{\epsilon R} - \frac{0.124e^4 \mu}{\hbar^2 \epsilon^2} = E_g^0 + \left| E_1 \left\{ \frac{\pi^2}{\xi} \left(\frac{a_0}{R} \right)^2 - \frac{3.572}{\epsilon} \left(\frac{a_0}{R} \right) - \frac{0.248\xi}{\epsilon^2} \right\} \right| \quad (1)$$

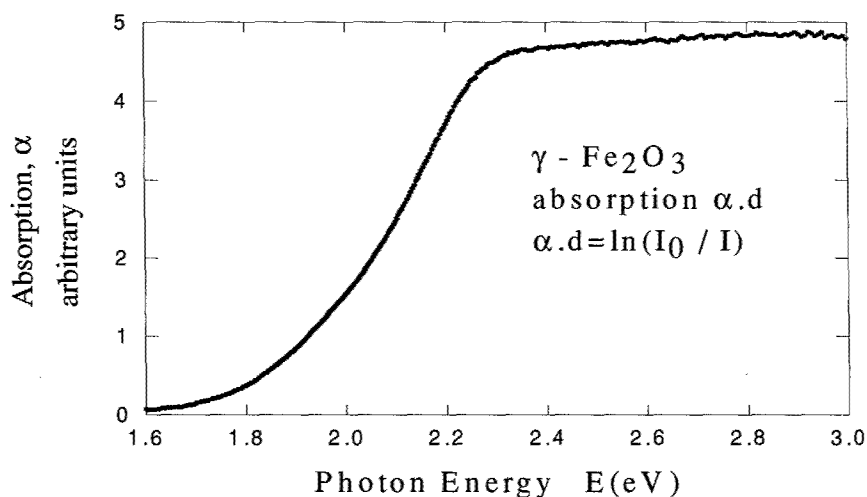


Fig.4. Optical absorption of 80 Å diameter particle size of γ -Fe₂O₃ nanocrystals

where E_g^0 is the bulk energy gap, ϵ is the dielectric constant of the material and

$$\mu = \frac{m_e^* m_h^*}{m_e^* + m_h^*}$$

is the reduced mass of the electron-hole pair. m_e^* and m_h^* are the effective masses of electron and hole, respectively. $|E_1| = \frac{1}{2} \frac{e^4 m_e}{\hbar^2} = 13.6 \text{ eV}$ is the hydrogen first excitation energy and

$a_0 = \frac{\hbar^2}{e^2 m_e} = 0.529 \text{ Å}$ is the hydrogen Bohr radius. The effective mass of a carrier in a

semiconductor material is a fraction of the free electron mass m_e , i.e. $\mu = \xi m_e$. If we take $\xi = 0.2$ which is a typical value for semiconductors and $\epsilon = 2.67$ the dielectric constant of the material taken from dielectric data, the red shift for a particle of the composite of average radius $R = 42.5 \text{ Å}$ is $\Delta E_g = 0.2 \text{ eV}$. The red shift varies between 0.1 and 0.2 eV by varying the values of ξ, ϵ up to 20%. For a composite of particle size distribution the success of the equation (1) to give the red shift dependence upon the particle size is impressive. An alternative explanation to the red shift has been attributed to the compression of the material due to the surface tension. The excess pressure increases with decreasing size of the nanoparticle causing reduction of the energy gap¹⁹.

The magnetic properties of the nanocomposite can be explained¹⁹ in terms of Neel's²⁴

theory of superparamagnetism and its generalization by Brown^{25,26}. According this theory, single magnetic domain particles of volume V are characterized by a blocking temperature $T_b = KV/25k_B$. Above this temperature the particles are superparamagnetic and their magnetic moments can rotate uninhibited. Below the blocking temperature the magnetic moments of the particles are frozen out. Because of the particle size distribution the composite will have an average particle volume corresponding to a blocking temperature, below which the system shows magnetic hysteresis. In our system this temperature is around 55 K.

ACKNOWLEDGEMENT

The work was supported in part by the Physics Department at Villanova University and by the National Science Foundation under the proposal No. P621, NSF/CHESS at Cornell Synchrotron. We thank the staff at CHESS for their valuable help.

REFERENCES

1. L. E. Brus, W. L. Brown, R. P. Andres, R. S. Averback, W. A. Goddard III, A. Kaldor, S. G. Louie, M. Moskovits, P. S. Peercy, S.J. Riley, R. W. Siegel, F. A. Spaepen, Y. Wang, *J. Mat. Res.*, **4**, 704 (1989).
2. *Research Opportunities for materials with Ultrafine Microstructures*, (National Academy, Alexandria, 1989).
3. *Science*, **254**, 1300 (1991).
4. K. Bittler and W. Ostertag, *Angew. Chem. Int. Ed. Engl.* **19**, 190, (1980).
5. P. Ball and L. Garwin, *Nature* **355**, 761 (1992).
6. G. D. Stucky and J. E. McDougall, *Science* **247**, 669 (1990).
7. L. Gunther, *Physics World*, December, pp.28-34 (1990).
8. R. D. McMichael, R. D. Shull, L. J. Swartzendruder, L. H. Bennett and R. D. Watson, *J. Magn. Mater.* **111**, 29 (1992).
9. R. E. Rosensweig, *Ferrohydrodynamics* (MIT Press, Cambridge, 1985).
10. R. F. Ziolo, U.S. Patent 4 474 866, 1984.
11. C. Kittel, *Phys. Rev.* **70**, 965 (1946); D. J. Dunlop, *Phys. Earth Planet. Inter.* **26**, 1 (1981).
12. C. P. Bean and J. D. Livingston, *J. Appl. Phys.* **30**, 120 (1959).
13. I. S. Jacobs and C. P. Bean, in *Magnetism III*, edited by G. T. Rado and H. Shul (Academic, New York, 1963), Chap. 6, and references therein.
14. E. M. Chudnovsky and L. Gunther, *Phys. Rev. Lett.* **60**, 661 (1988).
15. E. M. Chudnovsky and L. Gunther, *Phys. Rev. B* **37**, 9455 (1988).
16. A. J. Leggett, S. Chakravarty, A. T. Dorsey, M. P. A. Fisher, A. Garg, and W. Zuerger, *Rev. Mod. Phys.* **59**, 1 (1987).
17. P. M. Fauchet, C. C. Tsai and K. Tanaka, Eds. in *Materials Issues in Microcrystalline Semiconductors* (Materials Research Society, Pittsburgh, PA. 1990).
18. J. K. Vassiliou, V. Mehrotra, M. W. Russell and E. P. Giannelis, *Mater. Res. Soc. symp. Proc.* **206**, 561 (1991); R. F. Ziolo, E. P. Giannelis, B. A. Weinstein, M. P. O'Horo, B. N. Ganguly, V. Mehrotra, M. W. Russell, and D. R. Huffman, *Science* **257**, 219 (1992).
19. J. K. Vassiliou, V. Mehrotra, M. W. Russell, E. M. Giannelis, R. D. McMichael, R.D. Shull, and R. F. Ziolo, *J. Appl. Phys.* **73**, 5109 (1993).
20. H. Takey and S. Chiba, *J. Phys. Soc. Jpn.* **21**, 1255 (1966).

21. Y. Kayanuma, Solid State Commun. 59, 405 (1986); Phys. Rev. B 38, 9797 (1988).
22. M Hayashi, T. Iwano, H. Nasu, K. Kamiya, N. Sugimoto and K. Hirao, J. Mater. Res. 12, 2552 (1997); B. Yu, C. Zhu, and F. Gan, Opt. Mater. 7, 15 (1997).
23. T. Takagahara, Phys. Rev. B 47, 4569 (1993).
24. L. Neel, Rev. Mod Phys. 25, 293 (1953); Adv. Phys. 4, 191 (1955).
25. W. F. Brown, Jr., J. Appl. Phys. 30, 130 (1959); *ibid.*, 34, 1319 (1963).
26. W. F. Brown, Jr., in *Fluctuation Phenomena in Solids* (Academic, New York, 1964), p.37.